



NAZARBAYEV
UNIVERSITY

School of Engineering and Digital Sciences

Bachelor of Engineering in
Mechanical and Aerospace Engineering

**Computational Analysis of Fluid Structure
Interaction (FSI) in Horizontal Axis Wind
Turbines (HAWTs)**

(Final Capstone Project Report)

by

Diana Nurzhanova, Aruzhan Sataibekova, Zhanibek
Kussinov, and Madi Makshatov

Lead Supervisor: Prof. Yong Zhao

Co-Supervisor: Prof. Desmond Adair

May, 2024

Declaration

We, Diana Nurzhanova, Aruzhan Sataibekova, Zhanibek Kussinov, and Madi Makshatov , hereby declare that this report, entitled “Computational Analysis of Fluid Structure Interaction (FSI) in Horizontal Axis Wind Turbines (HAWTs)” is the result of our own project work except for quotations and citations which have been duly acknowledged. We also declare that it has not been previously or concurrently submitted for any other degree at Nazarbayev University or elsewhere.

Signature:

Four handwritten signatures in black ink, arranged horizontally. From left to right: a stylized signature, a signature that appears to be 'Aruzhan', a signature that appears to be 'Zhanibek', and a signature that appears to be 'Madi'.

Name: Diana Nurzhanova, Aruzhan Sataibekova, Zhanibek Kussinov, and Madi
Makshatov

Date: May 1, 2024

Acknowledgments

We would like to express our sincere gratitude to all those who have contributed to the completion of this capstone project.

First and foremost, we extend our deepest appreciation to our supervisor, Professor Yong Zhao, for his invaluable guidance, support, and feedback throughout this project. His expertise and encouragement have been instrumental in shaping this work.

We are also deeply grateful to our co-supervisor, Professor Desmond Adair, for his advice, encouragement, and expertise. His guidance has significantly contributed to the success of this project.

Special thanks are also due to the instructor of our course Professor Konstantinos Kostas. Your constructive criticism have been invaluable throughout this journey.

We would like to extend our appreciation to our fellow PhD student, Sagidolla Batay, for the meaningful discussions, encouragement, and support throughout this project. Your insights and feedback have been incredibly valuable.

Finally, we would like to thank Nazarbayev University for providing the necessary resources and conducive environment for the completion of this project.

Thank you all for your support and encouragement.

Abstract

Wind power plays a crucial role in the worldwide shift towards sustainable and renewable sources of energy. Wind turbine power generation performances made them a widely adopted method for electricity production, playing a crucial role in the world's energy resources. Accordingly, optimizing the wind turbine blade's design is essential for increasing wind turbine performance and reducing expenses. The main aim of this capstone project is to analyze the Fluid Structure Interaction of the HAWTs and to achieve the most effective design of the turbine, in terms of power generation performance and resource requirement by optimizing the blades using low fidelity methods.

In engineering and scientific studies, low-fidelity and high-fidelity simulation and optimization have become common concepts, especially in the field of wind turbine design and analysis. These concepts are essential in order to study computational structure and controlling the resource demand, as well as improving the operation of the turbines. This paper focuses on applying low-fidelity optimization techniques with QBlade, which is a commonly used open-source software for creating aerodynamic simulations of horizontal-axis wind turbines. A low-fidelity simulation can involve simplified fluid dynamics calculations and simplified structural models, in the context of wind turbine design, in order to forecast the turbine's effectiveness. Compared to the high-fidelity simulations, low fidelity simulations are economically and computationally reasonable. It means that, in the process of optimization of design parameters of the wind turbine more design alternatives are available in order to reach the most effective parameters.

Computational Analysis of Fluid-Structure Interaction (FSI) within Horizontal Axis Wind Turbines (HAWTs) will be studied on the NREL 5MW and NREL Phase VI turbine. In order to get the optimization results of these wind turbine blades, low fidelity optimization methods, such as Betz and Schmitz theories will be used.

Contents

Acknowledgments	ii
Abstract	iii
Contents	iv
List of Figures	v
List of Tables	vii
1 Introduction	1
1.1 Background Information and History	1
1.2 The Structure	2
1.3 Wind generation complications	2
1.4 Problem and Thesis Statement	2
1.5 Importance of FSI	3
2 Literature Review	4
3 Methodology	7
3.1 Wind Turbine Models	7
3.2 Low fidelity optimization methods	9
4 Results and Discussion	17
4.1 Rotor and Turbine BEM Simulation Analysis	22
4.2 FSI Simulation Results	25
5 Conclusion	34
Bibliography	36

List of Figures

3.1	External and Internal geometry of NREL phase VI	8
3.2	External and Internal geometry of NREL 5MW	9
3.3	Blade Element theory forces (QBlade, 2023)	11
3.4	Wake and blade structures within the LLFVW technique (QBlade, 2023)	12
3.5	Forces and moments computed on turbine (Drofelnik, 2018)	14
3.6	Schematic representation of HAWT in yawed wind condition (Drofelnik, 2018)	15
3.7	Co-rotational Beam Approach (Qblade, 2023)	16
3.8	Vizualization of Co-rotational Beam Approach (Qblade, 2023)	16
4.1	NREL phase VI airfoils shapes and parameters	17
4.2	NREL 5MW airfoils shapes and parameters	17
4.3	Lift, Drag and Moment coeff. vs AoA of NREL phase VI	18
4.4	Lift, Drag and Moment coeff. vs AoA of NREL 5 MW	18
4.5	Optimization profile of NREL Phase VI	19
4.6	Optimization profile of NREL 5 MW	19
4.7	Original and optimized NREL phase VI loadings	20
4.8	Original and optimized NREL 5 MW loadings	20
4.9	Mode types	21
4.10	Power coeff. vs TSR & Thrust coeff. vs TSR for NREL 5 MW	22
4.11	Power coeff. vs TSR & Thrust coeff. vs TSR for NREL phase VI	23
4.12	Power coefficient as a function of TSR for NREL phase VI	23
4.13	Power vs windspeed & Thrust vs windspeed for NREL 5 MW	24
4.14	Power vs windspeed & Thrust vs windspeed for NREL phase VI	24
4.15	Turbine Data for simulation	25
4.16	Wake modeling for simulation	26
4.17	Flowchart for one time step of the aeroelastic model (QBlade, 2023)	27
4.18	Representation of Aero-Elastic coupling approach (QBlade, 2023)	27
4.19	Structural Model of NREL 5MW	28
4.20	Wind Boundary condition	28
4.21	FSI Simulation for NREL 5MW	29
4.22	FSI Simulation for NREL phase VI	30
4.23	FSI Simulation for optimized chord length design	31
4.24	FSI Simulation for concurrently optimized design	31

4.25	Flapwise, Edgewise, Torsional Stiffness vs Length Blade for NREL 5MW	32
------	--	----

List of Tables

3.1	Airfoil profile data on NREL phase VI	8
3.2	Key Parameters of NRELpPhase VI	8
3.3	Airfoil profile data on NREL 5MW	8
3.4	Key Parameters of NREL 5MW	9
4.1	Material properties	21
5.1	Distribution of Tasks	35

Chapter 1

Introduction

1.1 Background Information and History

Concerns about global warming, pollution, and energy security have raised interest in creating renewable and environmentally conscious sources of energy including wind, solar, hydropower, geothermal, hydrogen, and biofuels as alternatives to fossil fuels. Wind energy has the potential to offer effective answers to the worldwide challenges climate change and the energy crisis. Wind turbines produce electricity by using the kinetic energy from the wind, which allows them to play a substantial role in addressing climate change and promoting a cleaner, more sustainable energy environment. The effective use of wind energy eliminates the emissions of CO₂, SO₂, NO_x and other harmful waste present in regular coal-fueled power plants, as well as the radioactive harms associated with nuclear power plants.[1]

The appearance and application of wind energy has its roots extending back to the time of presence of different ancient nations. Many researchers have claimed that the many ancient civilizations had their own methods of generating the wind energy. One of the most effective ways of wind energy applications was sailing. The oldest appearance of the sails used on the rafts appeared in about 4000 B.C. by the ancient Chinese people. They were recycling the garbage and using them to create liners in the oceans. Another appearance of the sailing boats, created by the old Egyptian people, was in the Nile River back in 3400 BC.[1]

Another example of the application of wind energy was the windmills. The very first windmills were captured in the Eastern Han Dynasty (25–220 AD). The windmills were mainly used for the water pumping and grain grinding purposes by the ancient nations. The horizontal axis windmills were extremely popular in recent civilization because of their high efficiency.[1]

Unlike other historical applications of wind energy wind turbines were created with the purpose of converting the wind energy to electricity. The earliest self-operated wind turbine was created in 1888 by Charles Brush. This type of wind turbine was able to reach a peak power of 12 kW. The sample for the modern wind turbines was designed and created in 1955 in Denmark and was named Gedser wind Turbine.[1] All of these historical inventions led to the massive application of modern wind turbines, which commonly have three blades and can work to generate a large amount of power. Generation of the wind happens from the motion of air through the variations of different pressure gradients. The

wind moves from high pressure areas to the low pressure areas. The speed of the wind is greater in the regions with broad atmospheric pressure gradients. It means that, as the wind speed is higher it could lead to greater wind power that is generated by the wind energy-converting devices.

1.2 The Structure

The key components of a wind turbine include the rotor blades, nacelle, tower, generator, and control systems. Rotor blades capture wind energy, the nacelle houses the generator and other vital components, and the tower provides height for enhanced wind capture. Wind turbines are broadly categorized into two types: Horizontal Axis Wind Turbines (HAWT) and Vertical Axis Wind Turbines (VAWT). HAWTs, the most common, have the main rotor shaft and generator at the top of the tower, while VAWTs have a vertically oriented rotor shaft.

1.3 Wind generation complications

Even though wind energy is one of the most effective and ecological types of renewable energy, it has its difficulties in the way of producing electricity from the wind. Main aspects of these complexities are uneven solar heating, Coriolis force and regional limitations. Firstly, the most crucial among these factors is the unevenness of solar heating. There are several reasons for the unequal distribution of solar heating across the surface of the earth. The following factor affects this problem: the location of the sun on the same plane as the sun; the 23.5 tilt of the axis of the earth and the topographic surface of the earth. Secondly, the earth's self rotation creates the Coriolis force which affects the vector of the motions in the atmosphere. The presence of Coriolis force leads to the deflection of the wind throughout the pressure gradient. Thirdly, the general structure and roughness of the earth's surface leads to sudden change of the wind speed because of the height of different surfaces.

1.4 Problem and Thesis Statement

A clean and efficient energy source must be used in action to fulfill the world's expanding requirements for renewable energy. A comprehensive analysis of renewable energy sources reveals the significance of the wind turbines to the power generated from the wind energy. One of the main factors influencing the capability of the wind turbine to generate the immense amount of power is the design of the blades. In order to create a sustainable energy source, the wind turbine blade requires being analyzed and optimized by using the

CFD simulation. Computational Fluid Dynamics (CFD) is a numerical analysis technique that can investigate the fluid and the flow of air within and around the body. CFD simulation results from many research studies show that, as the size of the blades increase it could lead to the problematic consequences in terms of deformation. It means that the extent of the airflow needs to be considered while determining the size of the blades for wind turbines. In this paper, as a possible method to prevent the deformation effects for the blades of the turbines, Fluid Structure Interaction (FSI) is considered to analyze the wind turbines' performance. In order to optimize and analyze the performance of the Horizontal Axis Wind Turbines, by designing the NREL 5MW and NREL phase VI wind turbines, Qblade software was used.

1.5 Importance of FSI

Over the last years, wind turbines have seen a significant increase in both power capacity and size. With as getting bigger in size the larger and more flexible blades are now more vulnerable to aeroelastic challenges that arise from the complex interactions between the moving air and the turbine structure, known as fluid-structure interaction (FSI). As the turbines spin, the force of the wind can curve the blades, and this bending can then affect how the wind flows around them. This cycle can cause serious stability issues for the turbine, such as edgewise vibration and flutter. It shows that FSI modeling that considers the blades' behavior is essential [2].

In order to effectively model FSI, one should measure both airflow calculations and structural dynamics. Aerodynamically, the BEM (blade element momentum) model is widely used because it makes a good balance between computational efficiency and accuracy. On the structural side, beam models and finite element analysis (FEA) are conventional methods for measuring the turbine's structural reactions to the forces exerted by the wind [2].

Chapter 2

Literature Review

The optimization of wind turbine blade design is an essential part in increasing power production and efficiency. In Ceyhan (2008) a tool using blade element momentum theory (BEM) coupled with a genetic algorithm was created to contribute in the aerodynamic design and optimization of wind turbine blades. This tool was designed to increase the blades for peak power output, considering factors such as wind velocity, rotational speed, the number of blades, and their radius. Optimization of twist and chord distributions of each blade element led to substantial improvements in power output by selecting optimum airfoil families from the database during the optimization process [3].

Lanzafame and Messina (2007) applied a genetic algorithm to optimize a winglet by focusing on design variables using an extrapolation technique. It allows to adapt the rotor design, including selecting turbine geometric features like rotor diameter, aerodynamic airfoil shapes, chord, pitch, and twist. It also contributes the assessment of blade forces, torque, and power on the rotor shaft. Additionally, it allows for the evaluation of turbine efficiency among different wind speeds [4].

Rasmussen et al. (2003) combined the BEM theory with the momentum theory to subdivide the blade into several elements to calculate loads. Aeroelastic codes within the wind turbine research has developed and the transition from simple treatments to more comprehensive aeroelastic models were emphasized. Aeroelastic models in detail needs to accurately predict loads and dynamic behavior considering the complex interactions between aerodynamics, structural dynamics, and control systems in wind turbines. The integration of 3D airfoil data in the BEM method is highlighted as an essential advancement, with different methods aimed for correcting 2D airfoil data to include three-dimensional and rotational effects. These advancements aim to increase the accuracy and efficiency of aerodynamic simulations in wind turbine design and optimization efforts [5].

Clifton-Smith and Wood (2007) used a method differential evolution to perform numerical optimization on the chord and twist distributions of small wind turbine blades. The resulting chord and twist distributions obtained through numerical optimization differed from analytical expressions based on traditional blade element theory, especially for blades operating at the Lanchester-Betz limit. Moreover, a new technique for tip loss correction was employed to test the impact of numerical optimization on the shape of the chord and twist distributions. Through the optimization process, they were able to significantly improve the starting time of the wind turbine by a factor of 20 without decreasing power production potential. By optimizing the chord and twist distributions in

combination with the tip speed ratio, they managed to increase the power coefficient by 10 percent while maintaining improvements in starting time [6].

Elfarra et al. (2014) focused on applying computational fluid dynamics (CFD) methods to study the aerodynamic performance of horizontal axis wind turbines (HAWTs). Several CFD studies in the literature have conducted 3D rotor flow simulations, with some researchers using full Navier-Stokes simulations of HAWTs. The accuracy of different simulation methods, including blade element momentum (BEM), vortex lattice method, and Reynolds-averaged Navier-Stokes (RANS) simulations, have been compared using experimental data from the national renewable energy laboratory (NREL) Phase II. The authors explored the use of blade tip geometric modifications, such as winglets, to increase the aerodynamic performance of turbine rotors and reduce sensitivity to wind gusts. The addition of winglets aims to decrease the induced drag of blades and improve overall performance [7].

Tahani et al. (2017) investigated the process of designing and increasing a horizontal axis wind turbine by applying the blade element momentum (BEM) theory with metaheuristic optimization techniques. The BEM methodology, frequently employed in the field of wind turbine engineering, calculates the axial and tangential forces exerted on the turbine's blades by including momentum theory with blade element theory. BEM theory was employed for a novel design approach, using local linearization of chord and twist as innovative design parameters. Through their optimization process, the authors demonstrated significant increase in the power coefficient of the optimized wind turbine geometry compared to the base geometry. Also, they showed the effectiveness of combining BEM theory with metaheuristic optimization algorithms for improving wind turbine performance. The results of the study emphasized the advantages of using computational methods such as CFD to optimize wind turbine designs, reducing costs and time associated with experimental testing results [8].

Liu, Chen, and Ye (2007) crafted a model for optimizing the rotor blades of horizontal axis wind turbines, aiming to maximize the annual energy production. To accomplish this goal of optimization, the researchers employed the extended compact genetic algorithm (ECGA) as their primary searching method. The results showed a significant improvement in aerodynamic performance, leading to a 7.5 percent increase in annual energy output when using the designed blades compared to the existing ones [9].

Muchiri et al. (2022) focused on designing and fabricating a vertical-axis wind turbine with magnetic repulsion and optimizing its performance through aerodynamic considerations and material selection. The research applied principles from both blade element and momentum theories to engineer wind turbine blades, considering key aerodynamic factors. These included rotor power, the tip speed ratio, torque, solidity, lift and power [10].

Sihag, Kumar, and Tiwari (2022) focused on the computational fluid dynamics (CFD)

validation and aerodynamic behavior analysis of the NREL Phase VI wind turbine. They utilized a numerical simulation approach to evaluate the effectiveness of different computational domains on torque calculation using the Reynolds-Averaged Navier-Stokes (RANS) model. They designed 3D models of the turbine blades and tested the aerodynamic characteristics of the wind turbine under different conditions. The study aimed to investigate the impact of different types on the wind turbine's performance and torque generation [11].

Perez-Becker et. al. (2020) focused on developing and implementing a lifting-line free vortex wake (LLFVW) method for modeling wind turbine aerodynamics. The rotor blade was separated into ring vortices at the chord position, forming a lifting line. By utilizing the Kutta–Joukowski theorem and airfoil polar data, the circulation of the vortices was calculated. The LLFVW method was implemented in the QBlade for simulating wind turbine flow. To model the free convection of the wake, a vortex core model was used to avoid singularities [12].

Chapter 3

Methodology

3.1 Wind Turbine Models

The term "NREL Phase VI" describes the sixth stage of wind energy research conducted by the National Renewable Energy Laboratory (NREL), which aims to enhance wind turbine performance and dependability through research and testing [13]. This includes increasing wind turbine system reliability, cutting wind energy production costs, and boosting wind turbine efficiency. It is a two-bladed horizontal axis wind turbine. In comparison with other wind turbine models, its total mass and complexity are decreased by using two blades, which might result in cheaper production as well as installation expenses. The National Wind Technology Center (NWTC) and NREL provide extensive testing, including wind tunnel examinations and field validation for assessing prototype wind turbines under real-life circumstances for NREL Phase VI wind turbines.

The NREL 5 MW wind turbine used in this project is a wind turbine developed by the National Renewable Energy Laboratory (NREL), a research center that focuses on developing energy efficient, sustainable, and renewable power technologies. This wind turbine can be defined as a horizontal-axis wind turbine (HAWT) and a conventional three-bladed upwind variable-speed variable blade-pitch-to-feather-controlled turbine. HAWT turbines that extract wind energy on horizontal axis and are parallel to the ground, are the most commonly used wind turbines due to their higher efficiency compared to VAWT turbines. The NREL 5MW was designed to generate a maximum power output of 5MW and to develop reference specifications for numerous research projects supported by the U.S. DOE's Wind & Hydropower Technologies Program [13].

3.1.1 Gross properties of NREL 5 MW and NREL phase VI

The NREL phase VI wind turbine has been determined only by S809 airfoil data [Table 3.1]. Other general parameters of rotor and hub are demonstrated on Table 3.2. The 5MW consists of three blades with a 63 m rotor radius that are defined by the following cross sectional profiles: DU21, DU25, DU30, DU35, DU40, NACA64 [14]. The key parameters on NREL 5 MW and airfoil data are shown in Table 3.3 & 3.4. The internal and external structures of both blades are presented on Figures 3.1 & 3.2.

Table 3.1: Airfoil profile data on NREL phase VI

Airfoil profile	Thickness [%]	Distance from the center [m]	Chord [m]
Circular Foil	100	2.00	3.542
NREL's S809 Airfoil	21	5.60	3.854

Table 3.2: Key Parameters of NRELpPhase VI

Items	Value	Units
Rated Power	19.8	kW
Cut-in Wind Speed	6	m/s
Cut-out Wind Speed	25	m/s
Rotor Diameter	10.058	m
Hub Height	12.192	m
Drivetrain	low-speed shaft, gearbox, and high-speed shaft	N/A
Tower mass	815.1	kg

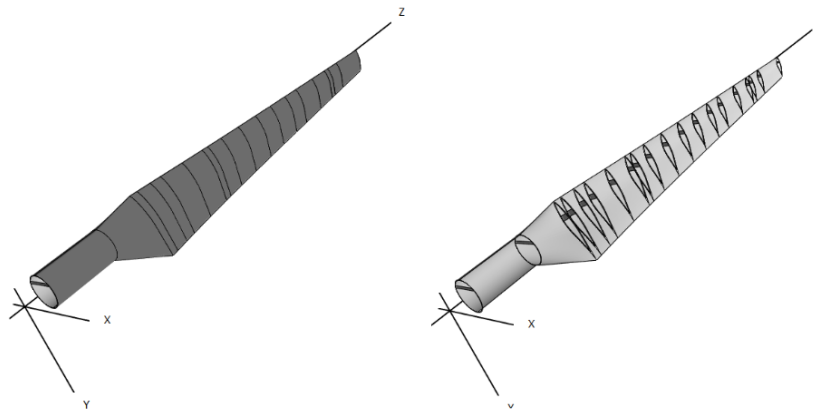


Figure 3.1: External and Internal geometry of NREL phase VI

Table 3.3: Airfoil profile data on NREL 5MW

Airfoil profile	Thickness [%]	Distance from the center [m]	Chord [m]
Cylinder 1	100	2.00	3.542
Cylinder 2	100	5.60	3.854
DU40-A17	40.50	11.75	4.557
DU35-A17	35.09	15.85	4.652
DU30-A17	30.00	24.05	4.249
DU25-A17	25.00	28.15	4.007
DU21-A17	21.00	36.35	3.502
NACA64-A17	18.00	44.55	3.010

Table 3.4: Key Parameters of NREL 5MW

Items	Value	Units
Rated Power	5000	kW
Rated Wind Speed	11.4	m/s
Cut-in Wind Speed	3	m/s
Cut-out Wind Speed	25	m/s
Rotor Diameter	126	m
Hub Height	90	m
Drivetrain	Multiple-Stage Gearbox	N/A
Tower mass	347460	kg

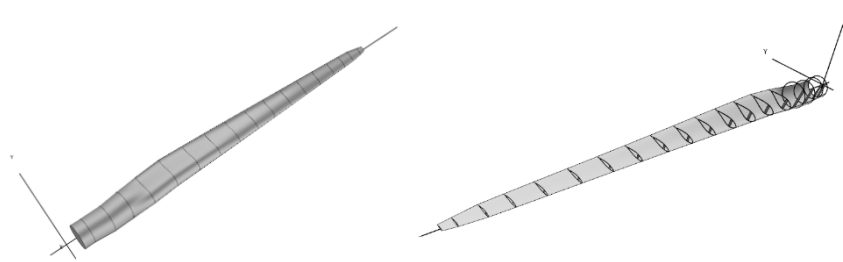


Figure 3.2: External and Internal geometry of NREL 5MW

3.2 Low fidelity optimization methods

The practice of optimizing a system or design applying simplified models or prototypes is referred to as low fidelity optimization [12]. One of the hardest and most essential processes in the creation of a wind turbine blade is designing its shape. Several hypotheses exist to forecast aerodynamic performance and determine the best chord and twist angle distribution. In QBlade software, 2 methods for blade's shape optimization according to the exact tip speed ratio were presented: Betz and Schmitz theories[15]. The objective of optimization is to reduce drag force and structural stress on the rotor and increase the amount of energy captured from the wind. The Schmitz approach uses quantitative optimization algorithms to find the optimal blade dimensions. Some examples of these algorithms include gradient-based procedures and evolutionary algorithms [6].

In terms of analysis of blade structure, the rotors of turbines are guaranteed to be able to sustain (aero)dynamic and gravitational loads while in use. To optimize the shape of blade and choice of materials for strength and long term usage, Finite Element Analysis (FEA) approaches evaluate the blade's fatigue life and stiffness. The overall wind turbine efficiency can be maximized through the use of CFD and BEM theory by modifying the rotor geometry and control techniques [7]. Aerodynamic loss reduction and collecting energy are achieved by optimizing design variables through descriptive research and repeated simulations. Tower design takes into account characteristics of the material, height and diameter dimensions to maintain the turbine and endure wind. Over

the wind turbine's lifetime, secure and reliable functioning is ensured by structural analysis procedures that assess load distribution and tower deflection.

3.2.1 QBlade software

In this project, all the simulations and blade design optimizations were performed using the QBlade software. Qblade is an advanced software developed for a wide range of applications, such as aero-servo-hydro-elastic development, prototyping, simulation, and certification of wind turbines QBladewebsite. The software was originally designed to join all the tools necessary for aerodynamic wind turbine design, simulation and to create a database on wind turbines. QBlade provides many tools to enable highly detailed simulations of wind turbines. Specifically, the Blade Element Momentum method can be utilized for the simulation of horizontal axis and a Double Multiple Streamtube (DMS) algorithm can be applied for the simulation of vertical axis wind turbine performance [16]. By utilizing this software, the Airfoil design and analysis, Lift and drag polar extrapolation, Blade design and optimization, Turbine definition and simulation can be performed which saves a numerous amount of time. The software was chosen primarily due to the algorithms that were integrated into it. For instance, the XFOIL algorithm based on potential flow theory generates or imports the airfoil polars to extrapolate them to the full range of 360° AoA. As for the Blade Design and Optimization, QBlade visualizes (via OpenGL) the blade and rotor design, the geometry by specifying the chord length, twist angle, edgewise or flapwise blade curvature, azimuthal angle and the twist axis of each individual airfoil [16]. For HAWT, the optimization can be performed after Shmitz or Betz. Overall, QBlade has gone through numerous validations by the research communities and successfully applied in a broad application and in the near future more advancements to enable more functionalities are planned.

3.2.2 BEM

Blade Element Momentum theory (BEM) is a theoretical framework extensively used in the field of wind energy to predict the performance and power production of wind turbines. It is a combination of Blade Element theory and Momentum theory [Figure 3.3].

The forces operating on a rotor may be calculated using the blade element theory by taking into account the geometrical and aerodynamic characteristics of each blade segment [17]. The blade is separated into portions that are dispersed radially in a defined number. Assuming that the flow is 2D, so the stresses on each section are computed. Momentum theory is based on the basic concept that airflow may be thought of as a system of stream tubes, all of them keeps its mass and momentum constant while circling a body. To make it easier, momentum theory states that the flow is irrotational and inviscid.

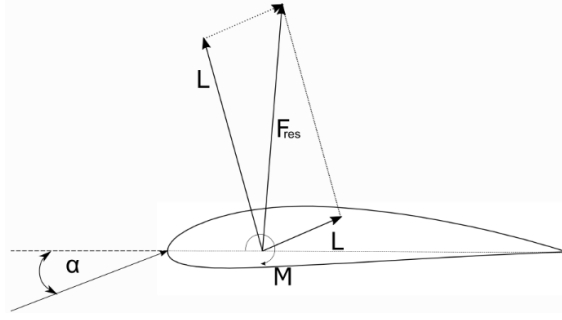


Figure 3.3: Blade Element theory forces (QBlade, 2023)

The main concept of BEM theory is breaking down the turbine blade into smaller segments and analyzing the aerodynamic forces acting on each of these elements. The blade force distributions are supplied by XFOIL, it is a 2D potential field solver [4]. However, this method applies only for stable flows that are evenly uniformed. BEM theory involves several calculations and formulas, here are some key equations used:

$$V_{rel} = \sqrt{(V_{wind} \cos \phi - v_{tangent})^2 + (V_{wind} \sin \phi)^2} \quad (3.1) \quad \text{{eq: relative windspeed}}$$

The efficient wind speed that a blade element experiences while it spins through the air is known as the local relative wind speed.

$$\alpha = \arctan \left(\frac{V_{rel} \sin \phi}{V_{wind} \cos \phi - V_{tangent}} \right) - \beta \quad (3.2) \quad \text{{eq: angle of attack}}$$

The angle of attack determines the angle at which the air hits the individual blade element. It's calculated based on the relative wind direction and the blade pitch angle.

$$L = \frac{1}{2} C_L \rho A_{ref} V_{rel}^2 \quad (3.3) \quad \text{{eq: lift force}}$$

$$D = \frac{1}{2} C_D \rho A_{ref} V_{rel}^2 \quad (3.4) \quad \text{{eq: drag force}}$$

The coupling of the flow of air and the blade surface produces lift and drag forces. These forces are computed using the lift and drag coefficients, which are properties of the airfoil design characteristics. The aerodynamic force needed to produce power is provided by the lift force, which operates perpendicular to the wind direction, whereas the drag force operates parallel.

$$T = \int_{r_{min}}^{r_{max}} (L \cos \theta - D \sin \theta) dr \quad (3.5) \quad \text{{eq: thrust force}}$$

The force that a rotor blades apply to the airflow while they revolve is known as the thrust force. In basic terms, it is the force that responds to the aerodynamic lift produced when the blades contact with the airflow. The integral accounts for the changing blade conditions across its length.

$$C_p = \frac{1}{2} \frac{T\omega r}{\rho A V_{wind}^3} \quad (3.6) \quad \{\text{eq:power coefficient}\}$$

The power coefficient is an important parameter derived from the proportion of the actual power obtained by the turbine to the maximum possible power that could be extracted from the wind passing through the rotor. It serves as an indicator of the turbine's effectiveness in transforming wind energy into mechanical power.

3.2.3 LLFVW

Lifting Line Free Vortex Wake (LLFVW) is a 3D potential flow field solver that also relies on XFOIL solver to generate dynamics of the wake at the back of blades [18]. It is a combination of Lifting Line theory and Free Vortex Wake. The LLFVW method in QBlade software can be used to simulate the aerodynamic forces operating on a rotor. The vortices on each rotor section located at 1/4 chord constitute a lifting line [Figure 3.4]. The primary distinction from the BEM theory is that the simulation resolves the rotor wake shed from the rotors [9]. The circulation can be calculated by using the Kutta-Joukowski theorem:

$$\Gamma = \frac{L}{V_{tot}} \rho = C_l(\alpha) \frac{1}{2} V_{tot} c \quad (3.7) \quad \{\text{eq:Kutta-Joukowski}\}$$

The incoming velocity, induced velocity and the velocity due to the motion of the rotor compose total velocity. By using the Biot-Savart Law, the induced velocity for each vortex element is determined:

$$V_{\Gamma}(x_p) = -\frac{1}{4\pi} \int \Gamma \frac{(x_p - x) dl}{(x_p - x)^3} \quad (3.8) \quad \{\text{eq:Biot-Savart law}\}$$

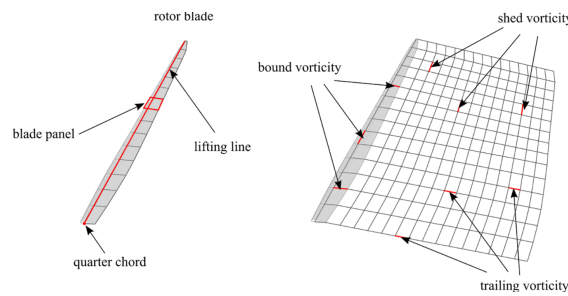


Figure 3.4: Wake and blade structures within the LLFVW technique (QBlade, 2023)

According to Marten et. al. (2023), applying a co-rotational method, the structural framework for the turbine in the QBlade-Chrono collaboration is constructed using Euler-Bernoulli beams [16]. The QBlade software program employs Chrono to carry out time-related simulations. The Fluid Structure Interaction (FSI) results were obtained by coupling LLFVW and Chrono.

3.2.4 CFD Modeling

Computational fluid dynamics (CFD) analysis is used to model the airflow around the rotors of wind turbines. In order to accurately represent the flow processes, this requires solving the Navier-Stokes equations (conservation of mass, momentum and energy), which characterize fluid flow behavior with the proper effect of turbulence:

$$\frac{\partial \rho}{\partial t} + \nabla(\rho u) = 0 \quad (3.9) \quad \{\text{eq:mass conservation}\}$$

$$\frac{\partial(\rho u)}{\partial t} + \nabla(\rho u u) = -\nabla \rho + \nabla \tau + \rho g \quad (3.10) \quad \{\text{eq: momentum conservation}\}$$

$$\frac{\partial(\rho E)}{\partial t} + \nabla((\rho E + p)u) = -\nabla(u\tau) + \nabla(q) + \rho u g \quad (3.11) \quad \{\text{eq:energy conservation}\}$$

Computational Fluid Dynamics is a detailed and flexible numerical modeling method, which allows the creation of a wide range of different scenarios, airflows, and turbine operational ranges for wind turbines. CFD is also highly effective in other engineering applications, such as water treatment, piping design for fluids, aerodynamic design for car, plane and ship hull design [15]. The development of CFD was then extended to the design of wind turbine blades and as a computer simulation tool for site assessment. CFD can be utilized to perform the flow analysis around the turbine and to validate the results the wind tunnel apparatus can be used for experimental purposes [15]. In case of wind turbines, the Blade Element Momentum theory is a low fidelity tool and CFD can be applied for more detailed aerodynamic analysis of the rotor of the oscillating devices and the conventional horizontal-axis wind turbines (HAWT) [16]. The high fidelity CFD method is the Navier-Stokes (NS) CFD, which is beneficial due to reduced uncertainty in flow predictions of low-fidelity models. Additionally, Navier-Stokes CFD is efficient in simulations of the flowfield of the wind farms, complex terrains, and wind conditions [16]. To perform CFD simulations the supercomputers which can withstand high loads are necessary and for that reason several sources on aerodynamic analysis of NREL 5MW and NREL Phase VI were reviewed. The CFD analysis was done based on research work performed by Drofelnik Jernej in 2018 at the Glasgow University, which presents the aerodynamic analyses and assessments results of HB RANS CFD code with the $\kappa - \omega$ SST turbulence model for the analysis of the NREL 5-MW baseline wind turbine [19]. According to this research, the forces and moments acting on the turbine with the tangential and axial force components of about $\pm 5\%$ and $\pm 6\%$ of their mean value, and with the torsional and in-plane bending moment of about $\pm 13\%$, and 11% of their mean value were analyzed.

Figure 3.5 demonstrates the forces and moments acting on the turbine.

The aforementioned forces acting on the blade were defined as following:

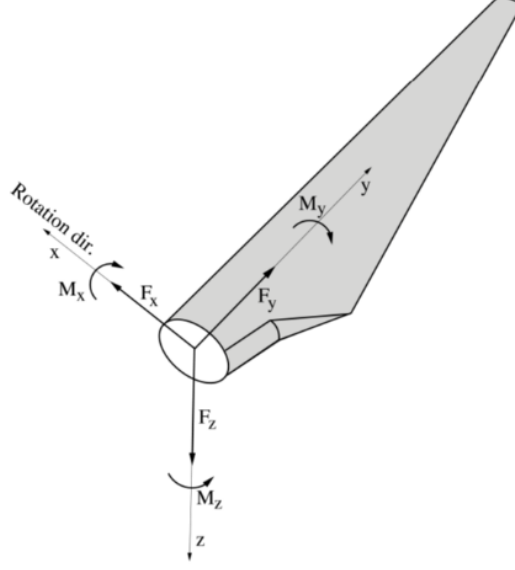


Figure 3.5: Forces and moments computed on turbine (Drofelnik, 2018)

$$F_x = \int_0^R F_{xy} dy \quad (3.12) \quad \begin{array}{l} \text{\{eq:} \\ \text{Tangential} \\ \text{force\}} \end{array}$$

$$F_z = \int_0^R F_{zy} dy \quad (3.13) \quad \begin{array}{l} \text{\{eq:Axial} \\ \text{force\}} \end{array}$$

On the blade section M_z , the exerted torque and moment are defined below:

$$M_{zy} = - \oint_S (\rho n dS) r_a + \oint_S (\tau n dS) r_a \quad (3.14) \quad \begin{array}{l} \text{\{eq:} \\ \text{Exerted} \\ \text{torque\}} \end{array}$$

$$M_z = \int_0^R M_{zy} dy \quad (3.15) \quad \begin{array}{l} \text{\{eq:} \\ \text{Moment\}} \end{array}$$

To analyze the performance of the turbine in unsteady conditions, the analysis of HAWT in yawed condition was done. The flow condition of yawed airfoils were affected by the freestream wind speed U_∞ , turbine rotational speed Ω , yaw angle δ , the angle between U_∞ and the normal to the rotor plane, chord c of the airfoil, and its distance r from the rotational axis. Referring to these parameters that impact the flow condition, the following scheme was created to represent the HAWT in yawed wind condition [Figure 3.6].

As a result, the circumferential and the axial components of the wind velocity on an airfoil was denoted as following:

$$\omega_z = u_\infty \cos(\delta) \quad (3.16)$$

$$\omega_\theta = \Omega R - u_\infty \sin(\delta) \cos(\Omega t) \quad (3.17)$$

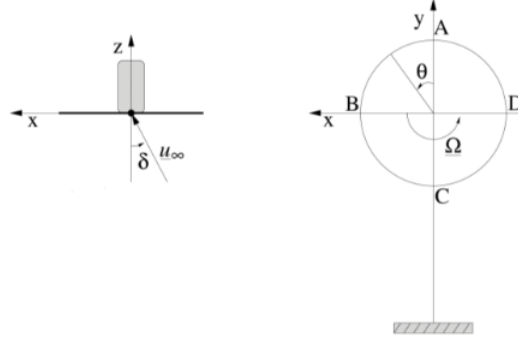


Figure 3.6: Schematic representation of HAWT in yawed wind condition (Drofelnik, 2018)

From these components of the velocity, the angle of the relative wind and the airfoil AoA α were defined below:

$$\phi = \arctan\left(\frac{\omega_z}{\omega_\theta}\right) \quad (3.18)$$

$$\alpha = \phi - \gamma \quad (3.19)$$

The variation in local AoA was caused by the induction of an inflow gradient by the velocity component.

3.2.5 Structural Dynamics (Project Chrono)

The FEA module from the open source software infrastructure, that is called Chrono project, is responsible for the structural model within the Qblade software [20]. A Project Chrono is a model based on physics and simulation tools built on a platform-neutral open-source design, coded in C++. Chrono has been modified to facilitate the modeling of linear and nonlinear finite element analysis (FEA) and fluid-solid interaction (FSI) problems. Specifically in Qblade software, Chrono::Engine module, which is practical for configuring and determining the physical structures with finite elements and Newtonian dynamics, is used. In order to solve finite element problems, The SparseLU solver, that is a part of the EIGEN C++ template library Tuxfamily is utilized. The Qblade source code includes the Chrono DLL, which has the information of Project Chrono and the EIGEN library. This makes it possible to define the physical system and the finite elements. It also gives the algorithm within the Qblade access to do time-domain simulation of structural dynamics.

The Euler Bernoulli beam co-rotational formulation defines the structural model of the turbines in Qblade-Chrono coupling. It can be seen in the figure that, in this co-rotational method, every deformable beam element is linked to a dynamic coordinate system. The movement of the beam element happens according to the rigid body's rotation and some strain deformation of the body in the moveable coordinate system. In Project

Chrono's operation, the overall tangent stiffness matrix is designed to incorporate elements accounting for geometric stiffness.

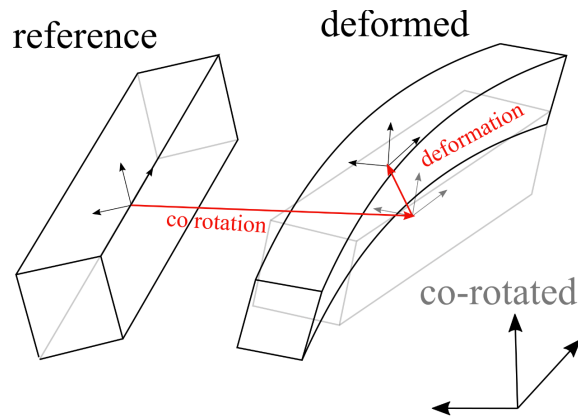


Figure 3.7: Co-rotational Beam Approach (Qblade, 2023)

Qblade software analyzes the wind turbine structure by fragmenting the parts of the turbine into separate bodies. In order to analyze the HAWT, Qblade software creates a separate body for every blade and one for the tower. Each of these bodies has their arrays for structural nodes and structural beam components. In addition, the software has more operations to define the positions, velocities, forces etc.

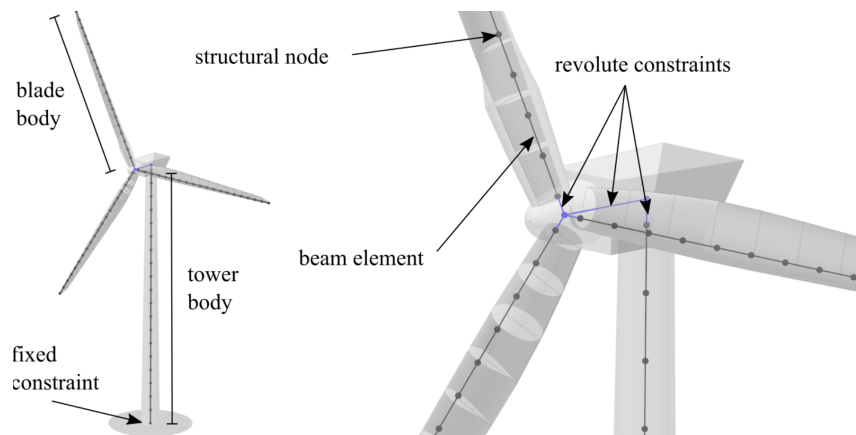


Figure 3.8: Visualization of Co-rotational Beam Approach (Qblade, 2023)

Chapter 4

Results and Discussion

Qblade software offers various tools to perform optimization of the blade design for several aims, such as increasing the power output, strengthening the structure or improving the overall aerodynamic performance of the turbine [15]. The optimization methods include following parameters: chord length and twist angle. By optimizing these parameters separately or simultaneously, the best outcome in accordance with the objective can be achieved. Our aim was to achieve the best power output after design optimization and for that aim Airfoil analysis, Steady BEM Analysis, Structural Blade Design and Analysis (QFEM), and the FSI Simulation of the wind turbines in QBlade software were performed. Comparing the power coefficients before and after optimization gave valuable insights on the aerodynamic performance of NREL Phase VI and NREL 5MW.

4.0.1 Airfoil Analysis

From the Figures 4.1 & 4.2 Airfoil Design Module, the shape of the airfoils are demonstrated and the user can adjust its parameters, such as thickness, camber, and location of maximum thickness.

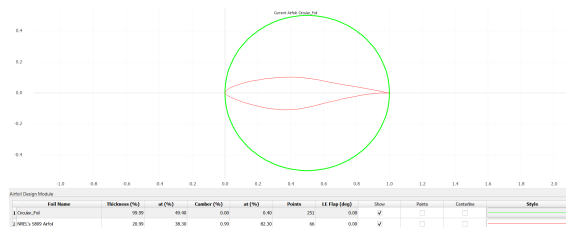


Figure 4.1: NREL phase VI airfoils shapes and parameters

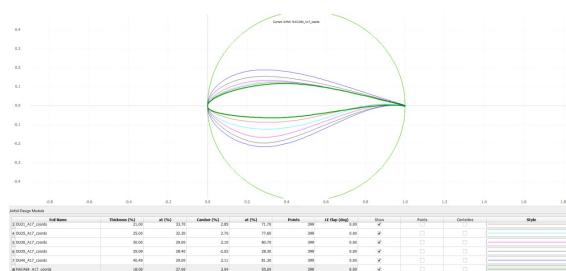


Figure 4.2: NREL 5MW airfoils shapes and parameters

This data is then used to analyze the aerodynamic performance parameters which are efficient in analyzing the optimization results. The aerodynamic study of 2D airfoil simulation was conducted to determine the lift, drag and pitching moment coefficient. Furthermore, stall characteristics and boundary layer analysis can be predicted.

For efficient extraction of power from the wind turbine the airfoil must generate more lift than drag. The lift force is perpendicular to the wind speed direction and due to the blade's shape, there is a pressure difference between the upper and lower surfaces which resulted in lift generation [9]. The maximum glide ratio C_l / C_d pointed at 6° angle of attack which means that optimized configuration increases the effectiveness of lift by minimizing the drag impact.

Choosing the NACA64-A17 profile as a polar, a Montgomery Polar Extrapolation to 360° was done to understand the aerodynamic behavior across the full operating range [Figures 4.3 & 4.4]. The polar definition was created with the dimensions: M (Mach number) = 0, Re (Reynolds number) = 10^6 and transition (laminar - turbulent) settings N -critical = e^9 . The polar curve is extended to higher angles of attack and the resulting graphs of lift, drag, moment coefficients can be used for performance prediction [21].

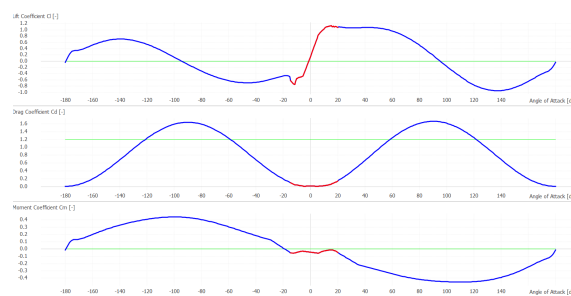


Figure 4.3: Lift, Drag and Moment coeff. vs AoA of NREL phase VI

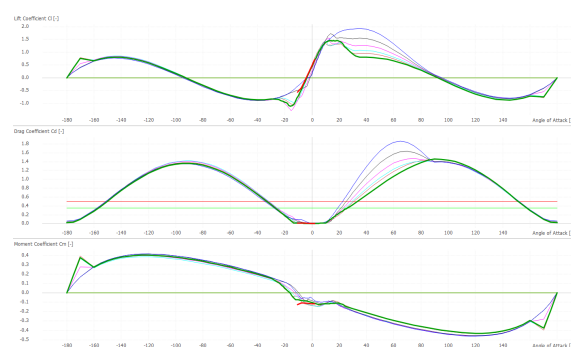


Figure 4.4: Lift, Drag and Moment coeff. vs AoA of NREL 5 MW

4.0.2 Steady BEM Analysis before and after optimization

In the HAWT Blade Design module in QBlade, the blade can be optimized by either the chord length or twist angle at a defined tip speed ratio. As for the first optimization method,

the chord length was optimized by applying the Schmitz method at TSR 6 (NREL phase VI) & TSR 6.6 (NREL 5 MW). As the second method, the twist angle was optimized at the same TSR. As for the last optimization, the chord length and twist angle were optimized concurrently. It needs to maintain a consistent tip speed ratio to ensure excellent performance over a broad range of wind speeds. The Schmitz method is done by narrowing the airfoil by pressing the top and bottom surfaces toward the chord line [8]. In QBlade software, tip loss reduction technique is also used: decreasing the creation of tip vortex and related losses by shifting the airflow from the blade's larger section to its narrower side. The change in chord length, twist angle before and after optimization can be seen from Figures 4.5 & 4.6.

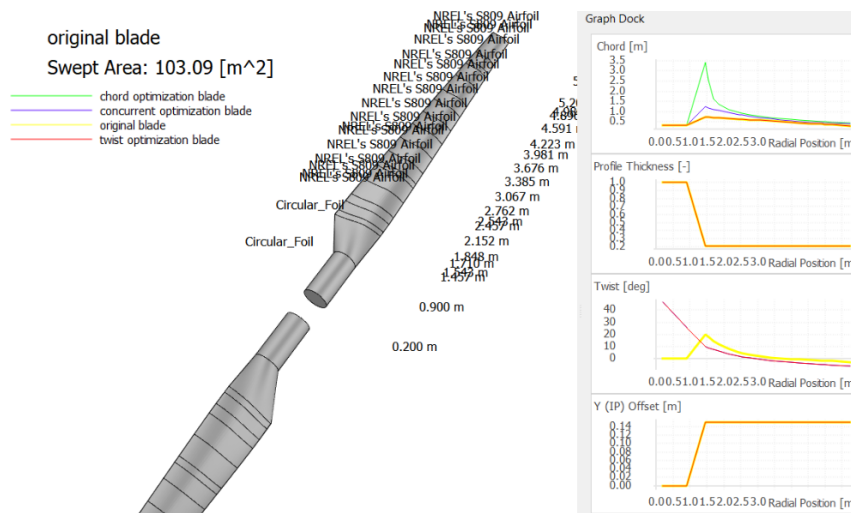


Figure 4.5: Optimization profile of NREL Phase VI

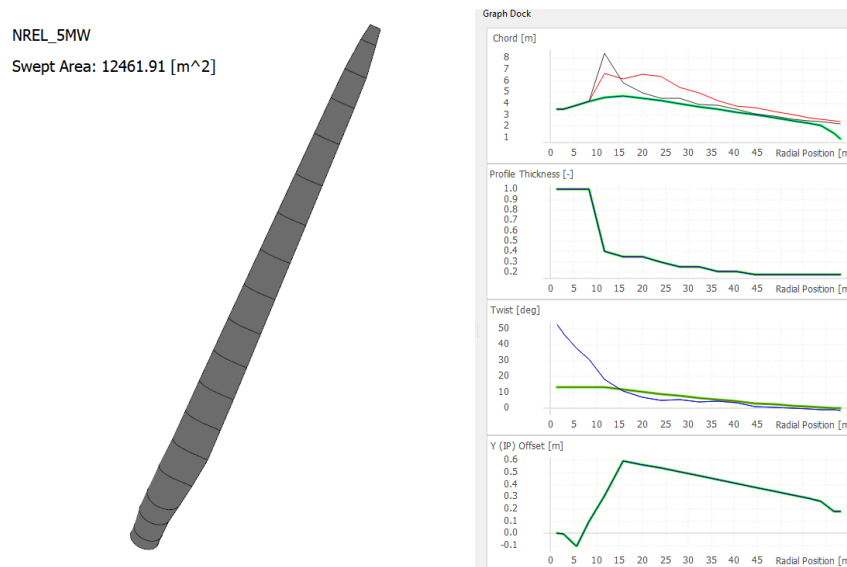


Figure 4.6: Optimization profile of NREL 5 MW

Quadratic - Finite - Element - Method (QFEM) analysis examined the structural blade design and static blade loading. For Fluid Structure Interaction (FSI) of NREL Phase VI wind turbine, the external material double bias was chosen, foam was selected as internal material. Due to its high strength and rigidity, dual-bias composites can sustain loads that are applied to the blade's outer surface [9]. In comparison with other standard materials, they demonstrate superior resistance to fatigue. Moreover, to minimize mass and inertia in rotors, these materials were selected because lightweight blades can react to changes in wind speed faster and need less energy in the beginning, which increases their total energy collection effectiveness. For NREL 5 MW wind turbine, the external material was chosen as 6000 series aluminium and for the internal material the triax fiberglass was chosen. The Structural integrity and behavior of the blades under different loading conditions were observed to understand the amount of stress and strain the blades can withstand. Overall, this analysis allows to explore the impact of optimization on the blade response to loads.

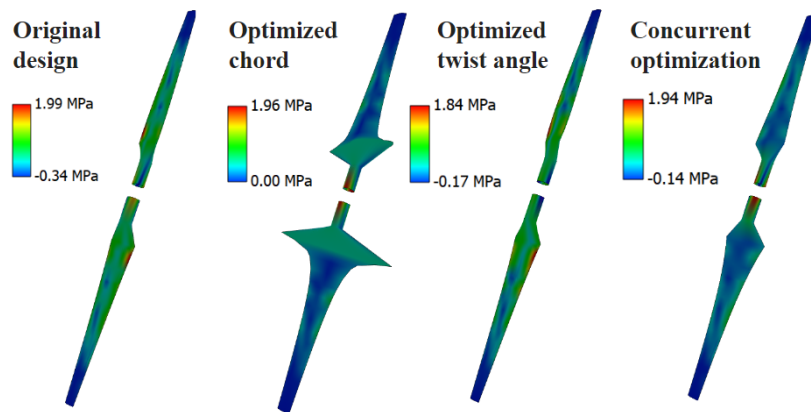


Figure 4.7: Original and optimized NREL phase VI loadings

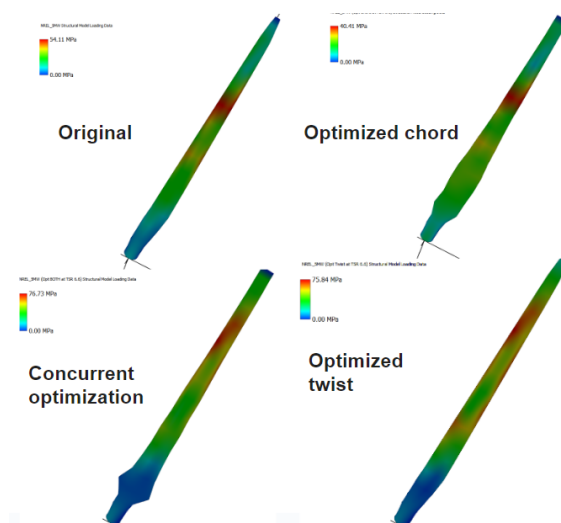


Figure 4.8: Original and optimized NREL 5 MW loadings

From the Blade Static Loading Figures the stress distribution across the blade can be evaluated. The adjustments made in chord length showed the uniform distribution of stress along the blade, while after optimization of twist angle only the stress concentration region was observed mainly around the middle section of the blade (See Figure 4.7 & 4.8). As for the optimization of both parameters, the stress distribution result was similar to the twist angle optimization result. As it can be seen from the magnitude of the stress acting on the blade, there is an increase in value. By adjusting either the twist angle only or concurrently with the chord length, the blade's capability of handling forces can be improved leading to better structural integrity and performance. With the help of understanding the stress distribution changes on modified design of the blade the optimal optimization method can be found.

Table 4.1: Material properties

Material	Elasticity modulus	Density
Double bias	$12 \cdot 10^9 \text{ Pa}$	1750 kg/m^3
Foam	$2.56 \cdot 10^8 \text{ Pa}$	200 kg/m^3
Triax fiberglass	$20 \cdot 10^8 \text{ Pa}$	1850 kg/m^3
Aluminium 6000 series	$70 \cdot 10^9 \text{ Pa}$	2740 kg/m^3

The blades of wind turbines may experience three different kinds of structural vibrations: torsional, edgewise, and flapwise [Figure 3.4]. The bending of the blade in the same wind flow direction (perpendicular to its longitude) is a flapwise mode. The term "torsional mode" describes how the blade twists (clockwise or counterclockwise with respect to its root) around its longitude. The bending in parallel direction to its longitude is known as edgewise mode [22]. During the static blade loading in QFEM analysis, normal and tangential loading applied to the blade [Figure 4.9].

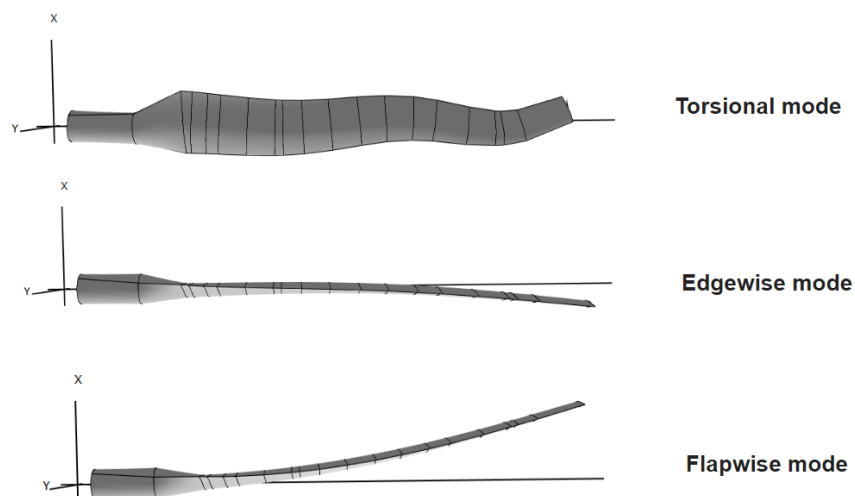


Figure 4.9: Mode types

4.1 Rotor and Turbine BEM Simulation Analysis

In this section, the impact of optimized design on blade's performance in terms of power and thrust coefficients will be analyzed. The power and thrust coefficients vs tip-speed ratio reveal some insights on which of the optimization methods show better power output. The resulting graphs can be seen from Figures 4.10 & 4.11.

Validation

It is noticeable from the thrust coefficient curves that the optimization of either twist angle or chord length enhances the rotor's efficiency in converting the wind energy into mechanical energy. Specifically, the optimization in terms of chord length and of both parameters demonstrated better results at lower TSR compared to the rotor with original design or with optimized twist angle design. Evaluation of how thrust coefficient changes after optimization may help to find the optimum range of TSR at which the conversion of wind's kinetic energy into mechanical energy is the most efficient. For both turbines, the maximum C_t occurred for concurrent optimization case.

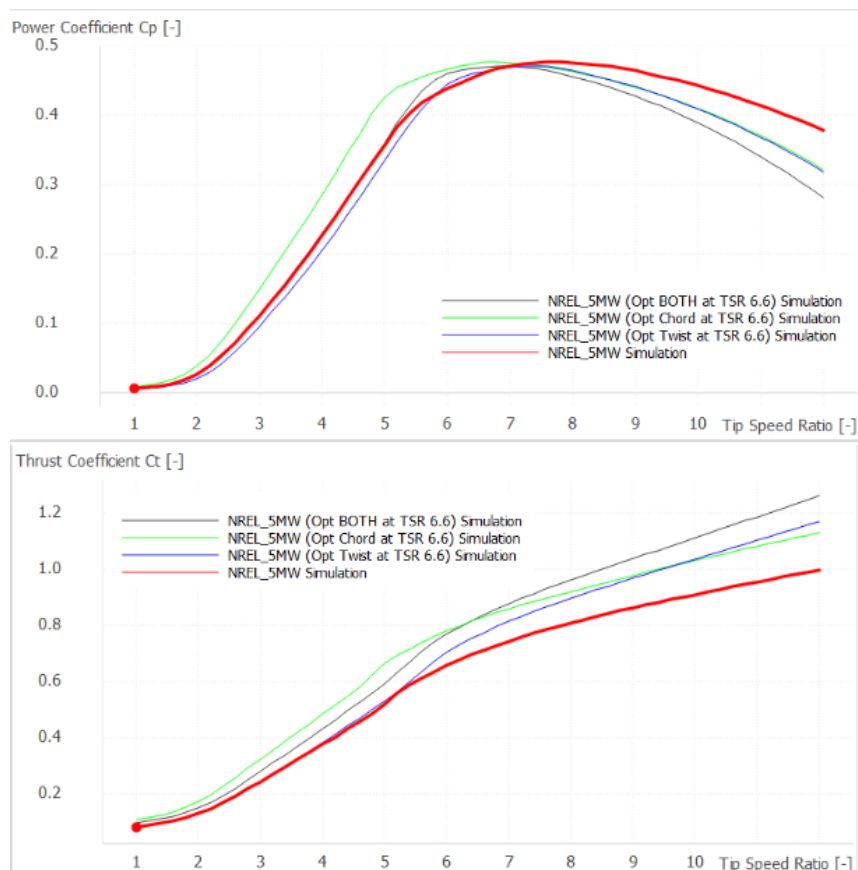


Figure 4.10: Power coeff. vs TSR & Thrust coeff. vs TSR for NREL 5 MW

As for the rotor's efficiency in extracting energy from the wind and converting it into electrical power, the Power coefficient vs Tip-Speed ratio figure was created. Similar to the case of thrust coefficient, the graph displays curves for each design. The curves for

chord length and concurrent optimization demonstrated that the power production of the rotor is better compared to the rotor with original design. The rotor with optimized design in terms of chord length reaches maximum power coefficient at lower TSR and this design can be prioritized over others if the aerodynamic efficiency and energy capture are chosen over other considerations.

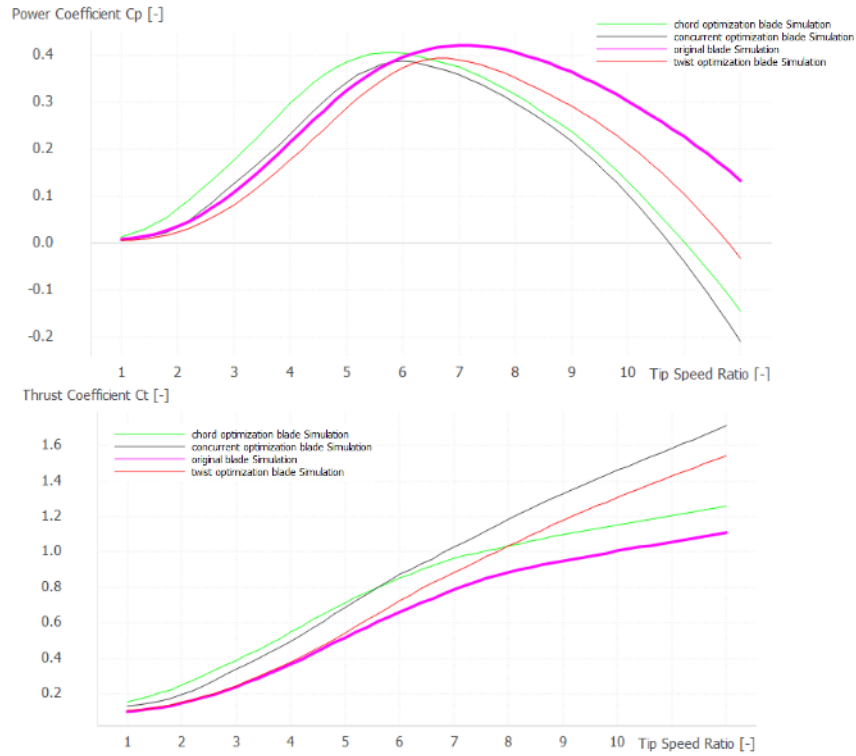


Figure 4.11: Power coeff. vs TSR & Thrust coeff. vs TSR for NREL phase VI

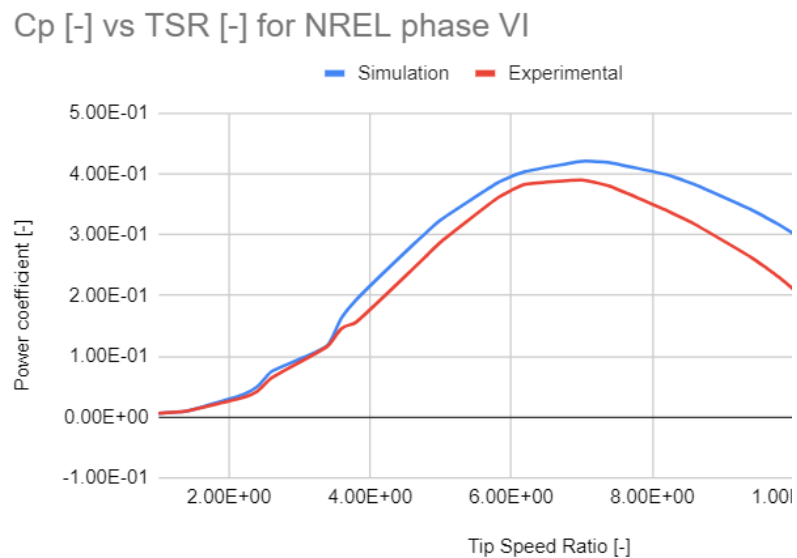


Figure 4.12: Power coefficient as a function of TSR for NREL phase VI

The Figure 4.12 demonstrates the compared results between simulation, which was done on QBlade and experimental from NREL report in terms of power coefficient VS tip-speed-ratio. For NREL 5 MW, the optimized chord length curve reached maximum C_p of 0.48 at TSR 6.6, while original curve reached C_p of 0.47 at TSR 7.6. For NREL phase VI, the original C_p was 0.43 at TSR 7, whereas optimized chord's C_p was 0.4 at TSR 6. Lower TSR values correspond to reduced centrifugal forces, dynamic loads and leading to better structural integrity due to lower rotational speeds of the blades. From the evaluation of thrust and power coefficient curves it can be concluded that optimization of chord length is more advantageous since it has more influence on wind energy harvest.

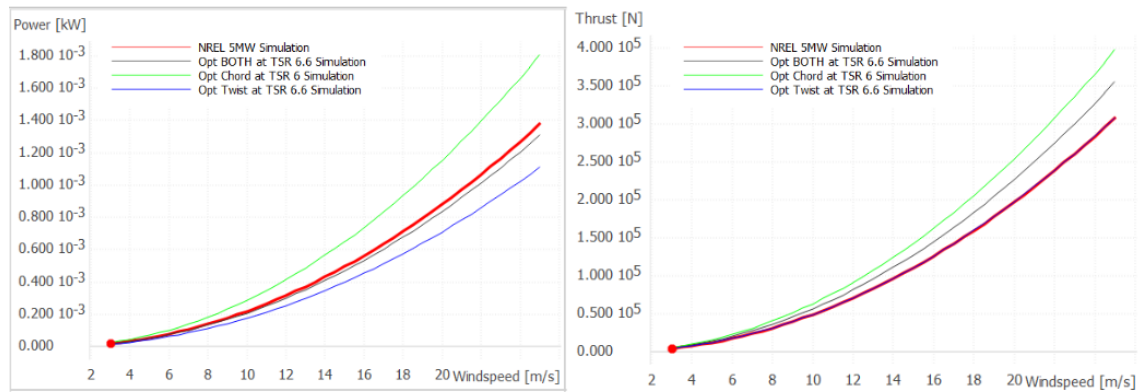


Figure 4.13: Power vs windspeed & Thrust vs windspeed for NREL 5 MW

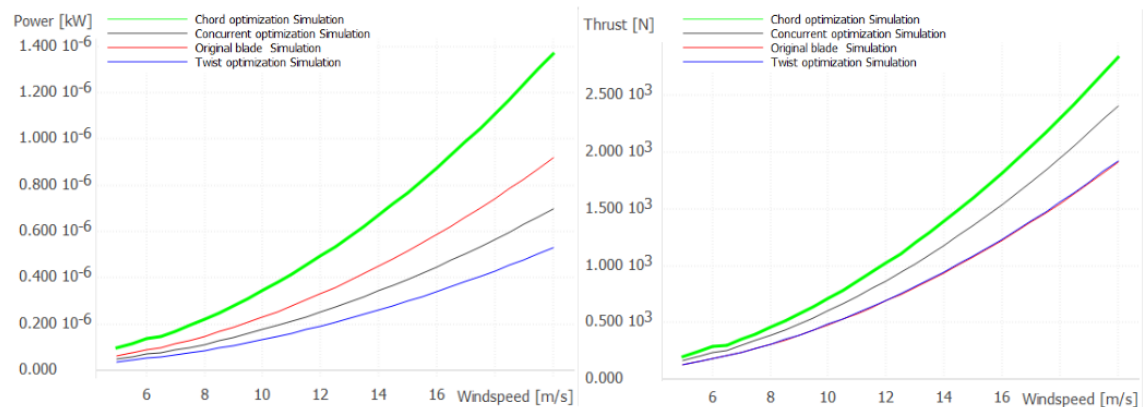


Figure 4.14: Power vs windspeed & Thrust vs windspeed for NREL phase VI

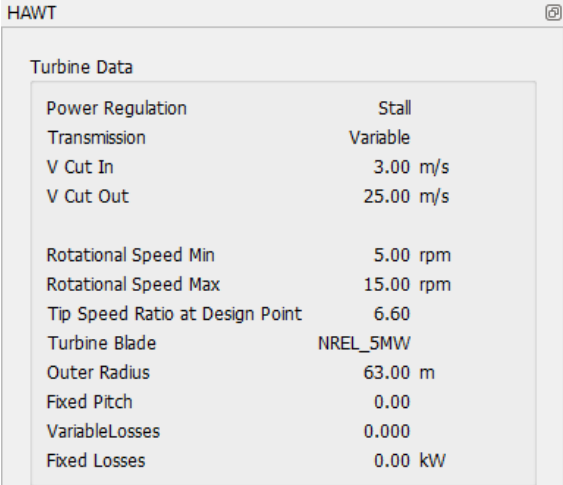
By evaluation of the power curves, the wind speed range at which the rotor can achieve its maximum power value can be determined [Figures 4.13 & 4.14]. The comparison of the curves demonstrate how the chord length optimization is more efficient in generating the highest amount of power throughout the whole range of wind speed. The design with optimized twist angle represented reduced efficiency in power generation. From the Thrust curves, the effect of the design changes on the turbine's ability to harness wind energy can

be assessed and the wind speed range at which the rotor reaches maximum thrust can be identified. Similar to the previous cases, the adjustments in chord length lead to generation of higher thrust under varying wind conditions. Additionally, the Thrust curves may help to assess the structural design requirements and this data will help to adjust the design that ensures the safety of the wind turbine. Overall, optimized design in terms of chord length yields higher power and thrust across different wind speeds and this results in enhanced performance of the wind turbine.

4.2 FSI Simulation Results

4.2.1 Turbine Definition

Before any simulation can be performed, the turbine should be defined and set up by specifying the turbine type and operational parameters [Figure 4.1]. The Power regulation was chosen as stall, which means that the power output is limited when a stall occurs at the rotor. As for the transmission, the optimum choice was variable to specify the maximum and minimum value for rotational speed and the desired TSR from which rotational speed is computed for every given wind speed during the simulation. The values for V Cut In and V Cut out are specified to show at which speed the turbine starts and stops. With defined parameters, the selected turbine with original design and optimized design can be added to the runtime database.



The screenshot shows a window titled 'HAWT' with a 'Turbine Data' section. The data is organized into two columns: parameter names on the left and their corresponding values on the right.

Turbine Data	
Power Regulation	Stall
Transmission	Variable
V Cut In	3.00 m/s
V Cut Out	25.00 m/s
Rotational Speed Min	5.00 rpm
Rotational Speed Max	15.00 rpm
Tip Speed Ratio at Design Point	6.60
Turbine Blade	NREL_5MW
Outer Radius	63.00 m
Fixed Pitch	0.00
VariableLosses	0.000
Fixed Losses	0.00 kW

Figure 4.15: Turbine Data for simulation

The next step is Aerodynamic Turbine Design to prepare for the aerodynamic modeling of a turbine design. After the geometry of the turbine is defined, the wake type is set as Free Vortex. The Lifting Line Free Vortex Wake method is beneficial due to improved accuracy compared to Unsteady BEM under conditions such as changing inflow speed or direction or floating wind turbines.

Wake Type

Wake Type: Unsteady BEM Free Vortex

Wake Modeling

Wake Integration Type: EF PC PC2B

Wake Rollup: On Off

Include Trailing Vortices: On Off

Include Shed Vortices: On Off

Wake Convection: BL HH LOC

Wake Relaxation Factor [0-1]:

Max. Num. Elements / Norm. Distance:

Wake Reduction Factor [0-1]:

Count Wake Length In: Revolutions Timesteps

Wake Zones N/1/2/3 in Revolutions [-]:

Wake Zones 1/2/3 Factor [-]:

Figure 4.16: Wake modeling for simulation

A simple 1st Order Euler Forward integration (EF) was chosen that sets the velocity integration method for the wake nodes and the convection velocity was selected as the mean boundary layer velocity.

As for the FSI Simulation, the structural model of the wind turbine needs to be obtained and loaded into turbine definition. The structural model relates to the mass, inertia, stiffness properties which are necessary for the structural simulation engine. In our case, the structure of the turbine was modeled by Project-CHRONO integrated into QBlade and the main file was assigned to a turbine. Basically, the structural model is based on the FEA module of the open source multi-physics engine Project Chrono [10]. With the help of Chrono DLL linked to QBlade's source code, the solver gets access to perform time domain simulation of structural dynamics (see Figure 4.16).

4.2.2 Aero-Elastic coupling

As the structural model of the wind turbine is integrated, the mechanical behavior of the structure and the airflow over the turbine blades can be simulated in QBlade. The interaction of structural and aerodynamic models of the wind turbine refers to Aero-Elastic Coupling, which reveals the structural response of the turbine to aerodynamic forces. The loose coupling approach employed for simulation can be seen in Figure 4.18.

Initially, the simulation starts at time $t=t_0$, and as the iteration begins, the wake-induced velocities for the rotor panels are calculated having the constant shape of the wake. Blade aerodynamics, lift and drag properties of blade panels, and other adjustments like Snel's correction are calculated iteratively. Referring to integration with Structural Dynamics, the simulation runs with a structural time step t_s , the forces and moments acting on blade panels are interpolated by lift, moment, and drag coefficients. The structural dynamics simulation comes to an end when the simulation time reaches $t=t_0+t$ [Figure 4.17]. Once this time is reached, the beam components will be mapped back onto the aerodynamic grid.

As for the update of wake, the unnecessary wake elements are either grouped or removed since the Lifting Line Free Vortex Wake method is used. The motion of the wake elements and the surrounding flow field impact the self-induced wake velocities and the accuracy of the wake representation is ensured by the update of vortex core sizes. The demonstration of how wake evolves because of the changes in the flow field and the movement of the rotor blades is possible since the positions of wake elements are advanced by a time integrator. Kutta condition is used to assign the circulation of the newly created wake elements, which leads to smooth and accurate flow around the trailing edge of the blades.

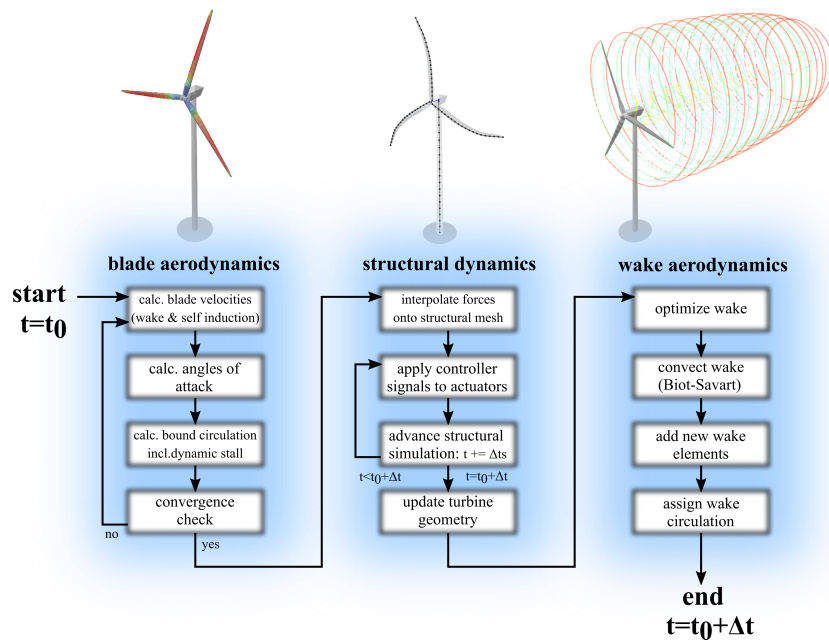


Figure 4.17: Flowchart for one time step of the aeroelastic model (QBlade, 2023)

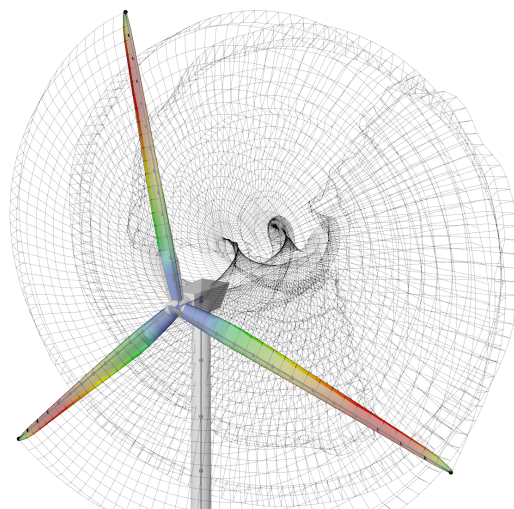


Figure 4.18: Representation of Aero-Elastic coupling approach (QBlade, 2023)

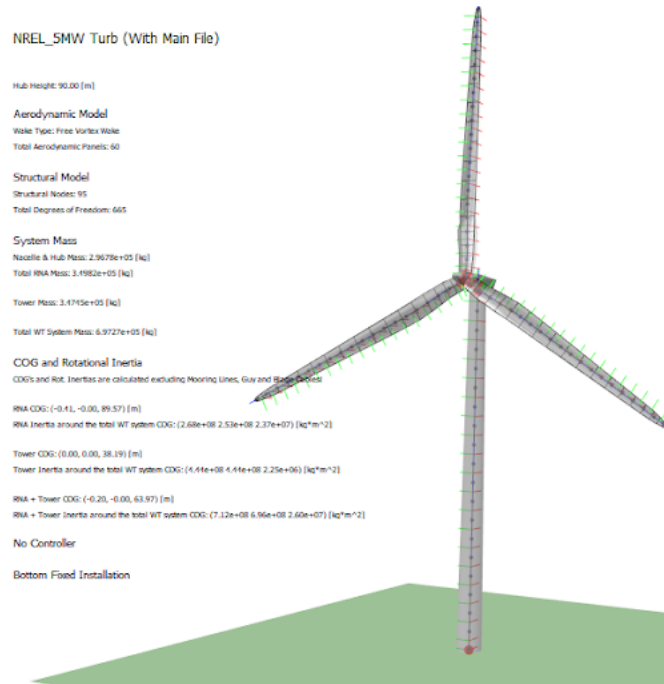


Figure 4.19: Structural Model of NREL 5MW

4.2.3 Simulation Module

In this section, the general simulation settings, wind boundary conditions, rotational speed settings, structural simulation settings, and turbine environment can be defined before the simulation results are obtained.

Wind Boundary Condition

Wind Input Type: Uniform Turbulent Field Hub Height File

Turbulent Windfields: Windfield

Turbulent Windfield Object: New Edit

Turbulent Windfield Shift [s]: Auto Manual 0

Turbulent Windfield Stitching: Periodic Mirror

Aerodyn Hub Height File: Load File

Windspeed [m/s]: 10

Vert. Inflow Angle [deg]: 0

Horiz. Inflow Angle [deg]: 0

Wind Shear Type: Power Law Log

Power Law Exponent [-]: 0.2

Roughness Length [m]: 0.01

Reference Height [m]: 110

Directional Shear [deg/m]: 0

Include Ground Effects: On Off

Figure 4.20: Wind Boundary condition

Most of the settings were set as default, except for wind boundary conditions. The Turbulent Field was selected as the Wind Input Type and the shift of the Windfield results by dividing the rotor diameter by the mean freestream velocity so that the rotor fully immerses at the start of a simulation. Since the Wind Input Type is Turbulent, the wind speed was set automatically as 10 m/s. All other parameters can be seen in Figure 4.20. The turbine environment was set as Onshore and environmental variables, such as Gravity, Air density, and Kinematic viscosity (Air) were set as default. As all parameters and definition settings are finished, the FSI Simulation of a wind turbine can be started. Selecting the necessary wind turbine and inserting windfield, the LLFVW coupled with Chrono for FSI simulation results are obtained.

FSI Simulation result for NREL 5MW and NREL phase VI

In Figures 4.21 & 4.22, the FSI simulation results for both wind turbines with the original design are demonstrated. These figures will be compared with others for optimized designs. Due to the small size of NREL phase VI wind turbine, the blade deformation may be unevident in relation to other elements under analysis due to the simulation's miniature scale.

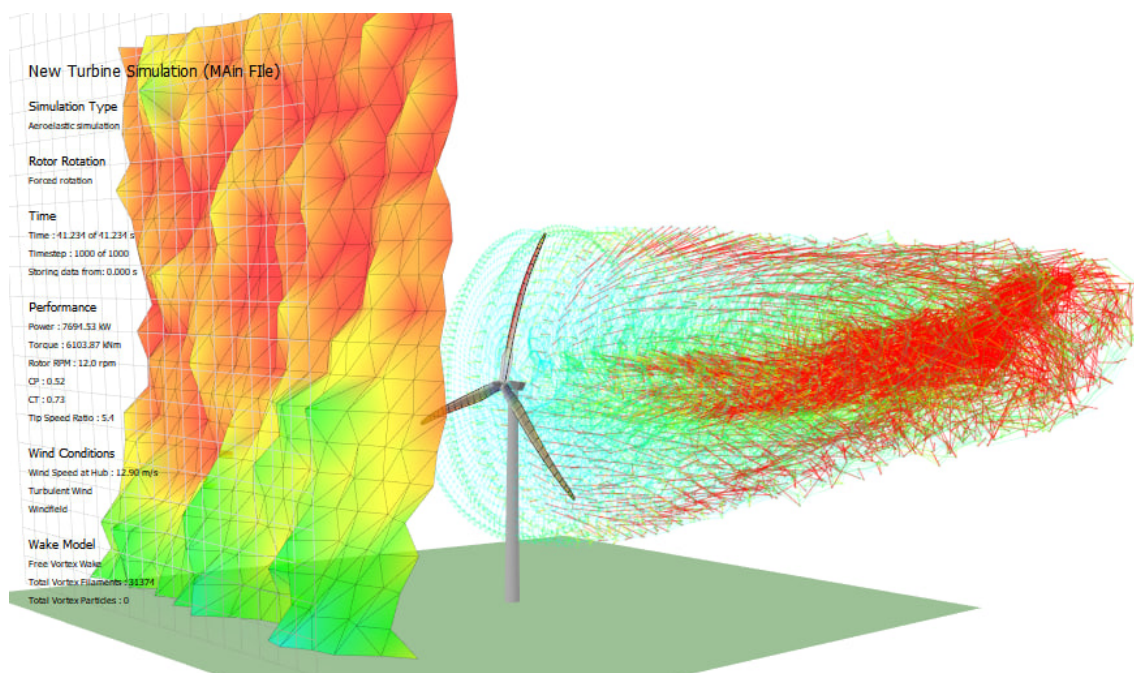


Figure 4.21: FSI Simulation for NREL 5MW

The resulting circulating distribution in the wake and the vorticity contour is demonstrated by color. From the figure, the wake geometry developed, and how the bound circulation formed around the blades can be observed. High positive trailing circulation was colored red, and negative trailing circulation was displayed in green. During low wind speeds, it is noticeable that at locations such as blade tip and root the wake the trailing circulation is concentrated, while during higher wind speeds, the trailing

circulation shifts into middle sections of the blades. The analysis of trailing vortices may help to gain information on the wake structure behind the turbine rotor [4]. The visualization of vortices allows for assessing the strength, size, and persistence of the wake which are valuable parameters for evaluating the downstream turbine performance. From large and persistent vortices the high levels of wake turbulence can be indicated and this is considered as an undesired impact on the efficiency and increase in structural loading. Moreover, the QBlade colors the wake by strain to demonstrate the distribution of strain or deformation in the wake field. The regions with high levels of strain signal increased turbulence and unstable flow. By analyzing the strain distribution the areas of concern can be identified.

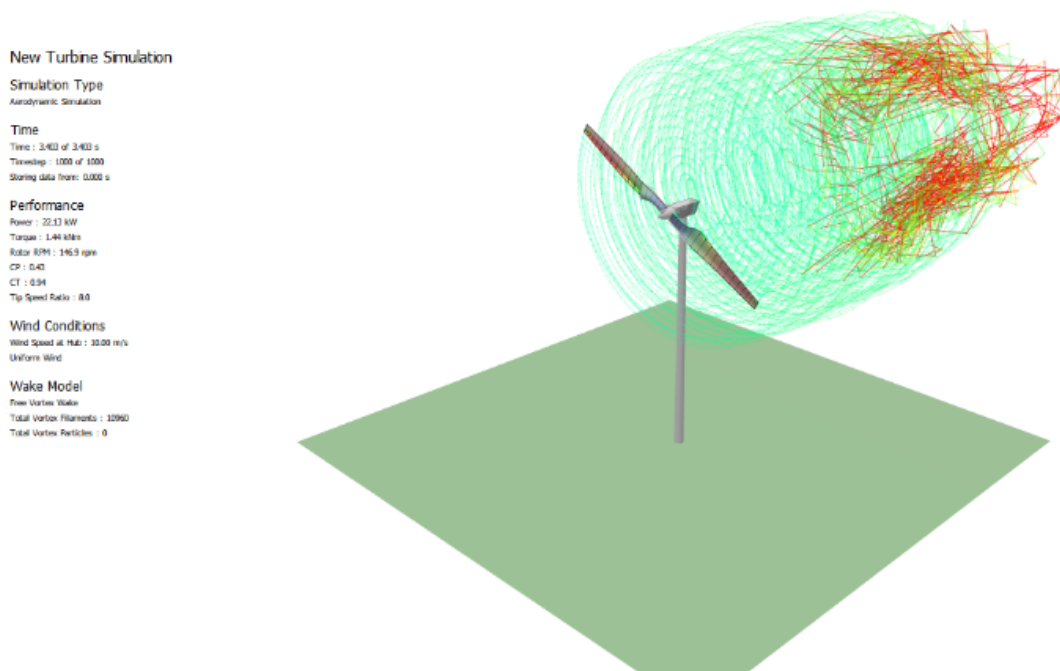


Figure 4.22: FSI Simulation for NREL phase VI

In addition, we can observe differences in the strength and shape of the vortices formed due to the contact between the blade and air around it. Referring to the vortices, the evaluation of their impact on the aerodynamic efficiency of the turbine can be performed by observing the lift distribution and flow separation. Due to the aerodynamic interactions the shed vortices, which show the rotational flow structures shed from the blades, are formed too. Consideration of vortex shedding is important to predict the loading and performance. Although chord length optimization is efficient in terms of power output, thrust coefficient and other general parameters of turbine performance, from FSI Simulation figures turbulence and instability in flow behind the rotor showed higher levels which might be a concern in terms of blade loading and fatigue.

As the FSI Simulation is done, the behavior of the blade under aerodynamic loads can be analyzed by the following graphs: Flapwise Stiffness, Edgewise Stiffness,

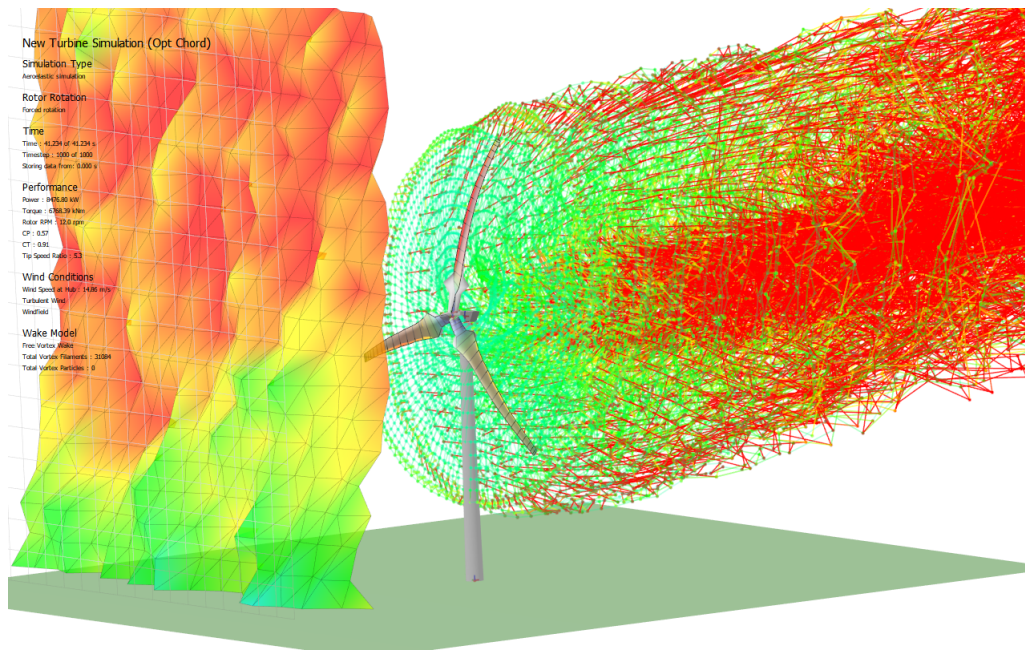


Figure 4.23: FSI Simulation for optimized chord length design

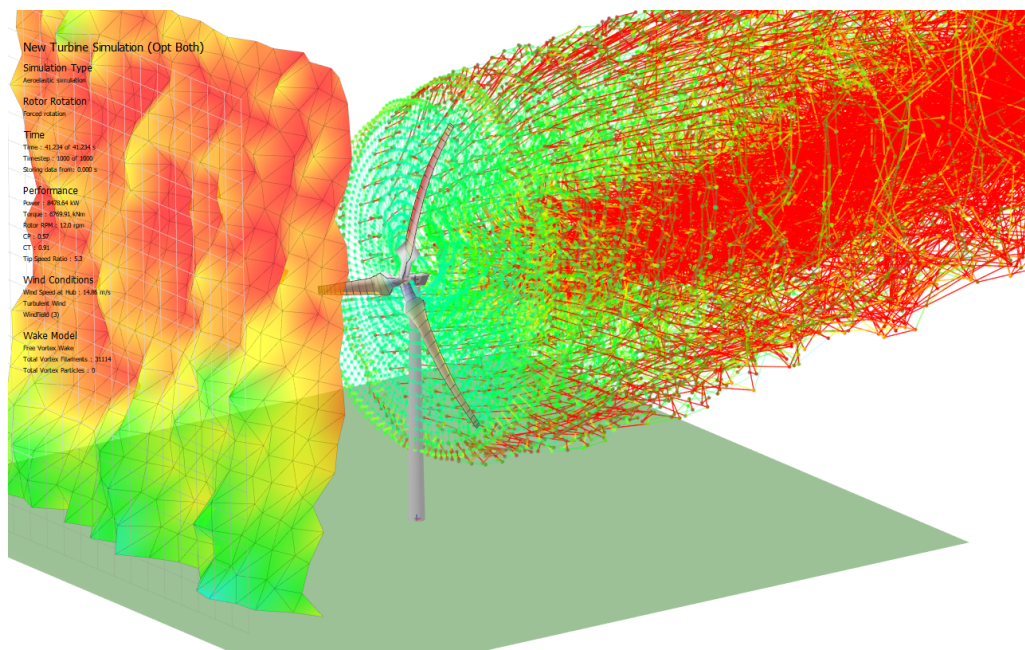


Figure 4.24: FSI Simulation for concurrently optimized design

Torsional Stiffness Distribution vs Length Blade. To understand the blade deflection under perpendicular to the rotor plane aerodynamic loads, the flapwise stiffness is important. If there is a high stiffness, it is a concern since it is desired to avoid excessive deflections which lead to fatigue. In another case, to observe the blade's response to loads, such as gravitational forces, when the blade is in the vertical direction, the Edgewise stiffness is essential. This is a concern in terms of the blade's ability to withstand loads without bending too much. The last, Torsional Stiffness, is crucial for understanding the blade's

resistance to twisting. To prevent aeroelastic instabilities such as flutter, it is necessary to have adequate torsional stiffness. The graphs for these factors are demonstrated by the Figure 4.25.

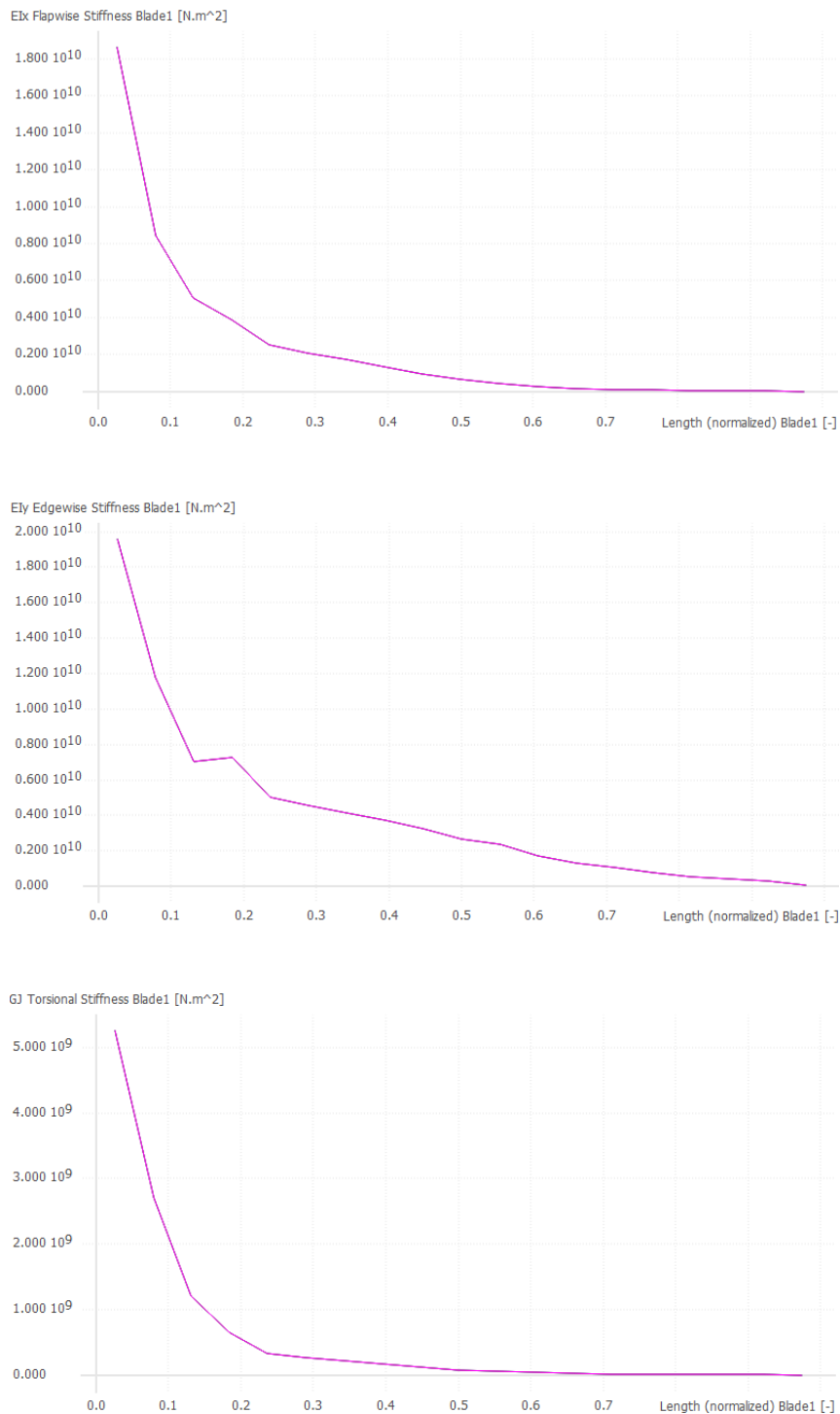


Figure 4.25: Flapwise, Edgewise, Torsional Stiffness vs Length Blade for NREL 5MW

From the 1st graph, a rapid decrease in Flapwise stiffness near the root can be observed. From the rapid decrease, it can be assumed that some regions of the blade are weak or more prone to bending deformation. Moreover, various material properties may contribute to

this decrease in stiffness since fiber orientation or laminate thickness leads to differences. In the second, Edgewise Stiffness graph, there is a steep decrease near the root followed by a more gradual decrease. It can be suggested that the blade optimization worked so that its ability to withstand different types of loads and stresses. The highest bending moments are typically at the root, and sufficient stiffness proves that the geometry of the blade is optimized. The pattern in the last, the Torsional Stiffness graph, is similar to the previous patterns of Flapwise and Edgewise Stiffness. A sharp decline near the root can be assumed as a flexible design of the blade's root to withstand stresses in this area. This parameter is important for the structural integrity of the blade since excessive twisting leads to mechanical failure. Variations are considered by engineers to understand how loads can be efficiently distributed and optimization of stiffness ensures the adequate response of blade aerodynamic forces. Generally, a smooth decrease near the tip in all three graphs can be assumed as a structural reinforcement performed to reduce weight and cost for the sake of structural integrity.

Chapter 5

Conclusion

In conclusion, this project has examined the low-fidelity fluid-structural optimization of horizontal axis wind turbine blades, along with their structural properties. The open-source software, Qblade was used to create aerodynamic simulation and blade optimization for the turbines. The main goal of this project was to reach the best power outcome as a result of design optimization of the blades. The optimization process was mainly based on the chord length and twist angle parameters. To reach our goal these parameters were optimized separately and jointly for both NREL 5MW and NREL Phase VI turbines.

First of all, the airfoil parameters of both of the wind turbines were analyzed. For NREL Phase VI, as the main airfoil profile NREL S809 airfoil was used. NREL 5MW turbines, in its turn, utilized NACA64-A17 airfoil as its main profile. The Airfoil profile data of both the turbines were described in Table 3.0 and Table 3.3, respectively. Secondly, turbines were optimized using chord length, twist angle, and concurrent optimization using the Schmitz method. In all of the methods, blades were optimized by TSR 6.0 for NREL Phase VI and TSR 6.6 for NREL 5MW. Chord length, and twist angle changes before and after optimization were demonstrated in Figures 4.5 & 4.6.

In the next stage, using the QFEM (Quadratic-Finite-Element-Method) analysis, static loading of the turbines was examined. The results for static loadings of NREL Phase VI and NREL 5MW are displayed in Figures 4.7 & 4.8, respectively. Following that, to validate the results of optimizations in terms of power and thrust coefficient, rotor and turbine BEM simulations were analyzed. The desired result after the optimization process was to get lower TSR values to get better structural integrity of the turbine. The results we were able to obtain after the validation are, for NREL Phase VI optimized chord's C_p was 0.4 at TSR 6, the original C_p was 0.43 at TSR 7, and for NREL 5MW the optimized chord length had maximum C_p of 0.48 at TSR 6.6, when an original curve reached C_p of 0.47 at TSR 7.6. Therefore, the obtained results after the validation of the optimized blades were successful.

Finally, after defining the turbine blades, the simulation of the turbines was performed in order to determine the dynamic FSI results. The dynamic FSI simulations of the turbines were performed with the original and optimized blades. As a result of these simulations, flapwise, edgewise, and torsional stiffness values vs the length of the blade are determined. From these results, it can be concluded that the highest bending occurs at the root of the blade, which proves the proper optimization of the geometry of the blade. Overall, the results after simulation can be interpreted as a structural strengthening intended to reduce

cost and weight without sacrificing structural integrity.

Generally, this project has demonstrated the effectiveness of using computational software like QBlade to improve the efficiency and reliability of HAWTs, using low-fidelity optimization and LLFVW methods. The results obtained from the FSI simulation have shown a significant impact on the wind turbine blades' aerodynamic performance and structural integrity. By using low-fidelity methods, we successfully optimized the NREL Phase VI and NREL 5 MW models, leading to better power generation and reduced structural loads. The results of this project lead to further developments in wind energy technology, encouraging the building of environmentally friendly and more efficient wind turbines. Advances in technology and additional research will ensure that the ideas shared here continue to influence the design plans for the future and promote the global utility of renewable energy sources.

Student name	Tasks
Aruzhan Sataibekova	Analysis of NREL 5MW wind turbine, QBlade simulations for NREL 5MW (Aeroelastic, FSI, BEM, Airfoil) Optimization of NREL 5MW blade design Methodology, Results
Diana Nurzhanova	Analysis of NREL Phase VI wind turbine, QBlade simulations for NREL Phase VI (Aeroelastic, FSI, BEM, Airfoil) Optimization of NREL Phase VI blade design Methodology, Results
Madi Makshatov	QBlade simulations for NREL Phase VI (FSI, BEM, Airfoil), Abstract, Introduction, Methodology, Conclusion
Zhanibek Kussinov	Introduction, Methodology, Literature Review parts in final Report

Table 5.1: Distribution of Tasks

Bibliography

- [1] W. Tong, “Wind power generation and wind turbine design,” 2016.
- [2] A. K. Lin Wang, Robin Quant, “Fluid structure interaction modelling of horizontal-axis wind turbine blades based on cfd and fea,” *Journal of Wind Engineering and Industrial Aerodynamics*, 2016.
- [3] O. Ceyhan, “Aerodynamic design and optimization of horizontal axis wind turbines by using bem theory and genetic algorithm,” *Middle East Technical University*, 2008.
- [4] R. Lanzafame and M. Messina, “Fluid dynamics wind turbine design: Critical analysis, optimization and application of bem theory,” *Renewable Energy*, vol. 32(14), p. 2291–2305, 2007.
- [5] F. Rasmussen, M. Hansen, K. Thomsen, T. Larsen, F. Bertagnolio, J. Johansen, H. Madsen, C. Bak, and A. Hansen, “Present status of aeroelasticity of wind turbines,” *Wind Energy*, vol. 6, pp. 213 – 228, 07 2003.
- [6] M. J. Clifton-Smith and D. H. Wood, “Further dual purpose evolutionary optimization of small wind turbine blades,” *Journal of Physics: Conference Series*, vol. 75, p. 012017, 2007.
- [7] M. A. Elfarra, S. U. Nilay, and I. S. Akmandor, “Nrel vi rotor blade: numerical investigation and winglet design and optimization using cfd,” *Wind Energy*, vol. 17(4), p. 605–626, 2014.
- [8] M. Tahani, T. Maeda, N. Babayan, S. Mehrnia, M. Shadmehri, Q. Li, R. Fahimi, and M. Masdari, “Investigating the effect of geometrical parameters of an optimized wind turbine blade in turbulent flow,” *Energy Conversion and Management*, vol. Volume 153, pp. Pages 71–82, 12 2017.
- [9] X. Liu, Y. Chen, and Z. Ye, “Optimization model for rotor blades of horizontal axis wind turbines,” *Frontiers of Mechanical Engineering in China*, vol. 2(4), p. 483–488, 2007.
- [10] K. Muchiri, J. Kamau, D. Wekesa, C. Saoke, J. Mutuku, and J. Gathua, “Design and optimization of a wind turbine for rural household electrification in machakos, kenya,” *Journal of Renewable Energy*, vol. 2022, pp. 1–9, 09 2022.

-
- [11] S. Sihag, M. Kumar, and A. Tiwari, "Cfd validation and aerodynamic behaviour of nrel phase vi wind turbine," *IOP Conference Series: Materials Science and Engineering*, vol. 1248, p. 012063, 07 2022.
- [12] S. Perez-Becker, F. Papi, J. Saverin, D. Marten, A. Bianchini, and C. Paschereit, "Is the blade element momentum theory overestimating wind turbine loads? an aeroelastic comparison between openfast's aerodyn and qblade's lifting-line free vortex wake method," *Wind Energy Science*, vol. 5, pp. 721–743, 06 2020.
- [13] National Renewable Energy Laboratory.
- [14] Airfoil Tools.
- [15] QBLADE - Next generation wind Turbine Simulation.
- [16] D. Marten, J. Peukert, G. Pechlivanoglou, C. Nayeri, and C. Paschereit, "Qblade: An open source tool for design and simulation of horizontal and vertical axis wind turbines," *International Journal of Emerging Technology and Advanced Engineering*, vol. 3, pp. 264–269, 2013.
- [17] W. Muhammad, S. Mohd, and B. Bambang, "The improvement of blade element momentum theory in horizontal axis wind turbine performance analysis," *Progress in Aerospace and Aviation Technology*, vol. 3, 12 2023.
- [18] G. Dejene, V. Ancha, and A. Bekele, "Nrel phase vi wind turbine blade tip with s809 airfoil profile winglet design and performance analysis using computational fluid dynamics," *Cogent Engineering*, vol. 11, pp. 1–21, 12 2023.
- [19] J. Drofelnik, A. Da Ronch, and S. Campobasso, "Harmonic balance navier–stokes aerodynamic analysis of horizontal axis wind turbines in yawed wind," *Wind Energy*, vol. 21, 01 2018.
- [20] A. Tasora, R. Serban, H. Mazhar, A. Pazouki, D. Melanz, J. Fleischmann, M. Taylor, H. Sugiyama, and D. Negrut, "Chrono: An open source multi-physics dynamics engine," 2016.
- [21] K. Lee, Z. Huque, R. Kommalapati, and S. Han, "Fluid-structure interaction analysis of nrel phase vi wind turbine: Aerodynamic force evaluation and structural analysis using fsi analysis," *Renewable Energy*, vol. 113, pp. 512–531, 12 2017.
- [22] K. Gaetan and J. R. Martins, "Aerostructural shape optimization of wind turbine blades considering site-specific winds," 12th AIAA/ISSMO Multidisciplinary Analysis and Optimization Conference, 2008.